

* * *

THE NEW WEDGE-SHAPED HUBBLE DIAGRAM OF 398 SCP SUPERNOVAE
ACCORDING TO THE EXPANSION CENTER MODEL

ECM paper IX by Luciano Lorenzi

54th Annual Meeting of the Italian Astronomical Society - Naples 2010

"L'Astronomia italiana: prospettive per la prossima decade"

ABSTRACT

Following the successful dipole test on 53 SCP SNe Ia presented at SAIIt2004 in Milan, this 9th contribution to the ECM series beginning in 1999 in Naples (43th SAIIt meeting: "Revolutions in Astronomy") deals with the construction of the new wedge-shaped Hubble diagram obtained with 398 supernovae of the SCP Union Compilation (Kowalski et al. 2008) by applying a calculated correlation between SNe Ia absolute blue magnitude M_B and central redshift z_0 , according to the expansion center model. The ECM distance D of the Hubble diagram (cz versus D) is computed as the ratio between the luminosity distance D_L and $1 + z$. Mathematically D results to be a power series of the light-space r run inside the expanding cosmic medium or Hubble flow; thus its expression is independent of the corresponding z . In addition one can have $D = D(z, h)$ from the ECM Hubble law by using the h convention with an anisotropic H_X .

It is proposed to the meeting that the wedge-shape of this new Hubble diagram be confirmed independently as mainly due to the ECM dipole anisotropy of the Hubble ratio cz/D .

1. Introduction

After the successful test of the expansion center model (Lorenzi 2004) carried out on 53 high-redshift Type Ia supernovae from the Supernova Cosmology Project (SCP: Perlmutter et al. 1999 or P99; Knop et al. 2003 or K03), here is presented the ECM construction of the new wedge-shaped Hubble diagram obtained by data from the SCP Union Compilation (Kowalski et al. 2008). In particular this large "Union" sample reports redshifts and blue magnitudes of 398 SNe Ia, or of 307 SNe Ia after selection cuts, including the distant supernovae recently observed with HST.

Let us remark that the cited papers I-II-III-IV-V-VI-VII-VIII are those of the author's references: Lorenzi 1999→2009.

2. Distances from the ECM equation

The **new Hubble law** (59) of paper I

$$\dot{r} = r \cdot (H + \Delta H) - R\Delta H \cos \gamma \quad (1)$$

, after substituting $H = H_0 + \Delta H$, ΔH , R with the formulas (37)(39) from paper I, becomes the **ECM \dot{r} equation** (from eq. (3) in paper II) of the nearby Universe, expressed in Hubble units (H.u.) as follows

$$\dot{r} = H_0 \cdot r \left(\frac{1+x}{1-x} \right) \left[1 + 3q_0 \frac{(1-x)^{\frac{1}{3}}}{1+x} \cos \gamma \right] \quad (2)$$

with

$$x = \frac{3H_0 r}{c} < 1 \quad q_0 = -\frac{H_0 R_0}{c} \quad \cos \gamma = \sin \delta_{VC} \sin \delta + \cos \delta_{VC} \cos \delta \cos(\alpha - \alpha_{VC})$$

being

$$K_0 R_0 = a_0 = -3H_0 q_0$$

Specifically γ is the angle between the direction ($\alpha_{VC} \approx 9^h, \delta_{VC} \approx +30^0$) of the huge void center (Bahcall & Soneira 1982), also called the expansion center or Big Bang central point (Lorenzi 1989-91-93), distant R_0 from the Local Group (LG) at our epoch and that (α, δ) of the observed outer galaxy/group/cluster/supernova at a distance r from LG, with the nearby Universe radial velocity \dot{r} corrected only by the standard vector (Sandage & Tammann 1975a)(Lorenzi: paper I).

Of course $\Delta H = 0$ in eq. (1) should give the original Hubble law: $\dot{r} = H_0 r$.

Here it should be noted that the above equation (2) allows us to define at least three different cosmic distances, the following r , D and D_L , which in practice have approximately the same value only for the very nearby Universe.

2.1 r : Distance as light-space

First of all the distance r in eq. (1) and (2) represents the light-space run with constant speed c inside the expanding "cosmic medium" (CM hereafter) or Hubble flow. In particular such a CM flow refers to the motion of galaxies running away from the Big Bang central point, with radial velocity $\dot{R} = HR$ (cf. papers I, V and VIII). Let us rewrite the **light-space** r formulation.

$$r = -c(t - t_0) \quad \text{with} \quad -c = \frac{\delta r}{\delta t} \quad (3)$$

In eq. (3) t_0 is a constant representing our epoch, which is also represented by $r = 0$; at t_0 the light emitted at an epoch t reaches the observer at rest in the local Hubble flow, which now is more rarefied like the CM; δr is the infinitesimal CM space covered by the light during an infinitesimal δt of the light travel-time from the past. To all intents and purposes the source distance r of eq. (3) may be considered to be equal to that of the source at the emission epoch t . However the cosmic medium is expanding, while light speed c remains constant with respect to the local cosmic medium, as follows: $\lambda = cT \Rightarrow d\lambda = cdT \Rightarrow \lambda + \Delta\lambda = c(T + \Delta T) \Rightarrow \lambda_0 = cT_0$. In other terms the travelling light has two speeds, the former being c inside CM, the latter that of the supporting expanding CM or Hubble flow. The observed velocity of this expanding CM is the derivative of r to t , with $dt_0/dt \equiv \lambda_0/\lambda$ assumed, as shown in papers V and VIII, sections 4.7 and 2.1 respectively. That dr/dt results to be $c\Delta\lambda/\lambda$, that is $\dot{r} = cz$. By introducing z in eq. (2) we obtain the dimensionless **ECM z equation** (eq. (22) of paper V or eq. (13) of paper VI or eq. (6) of paper VII)

$$z = \frac{x}{3} \left(\frac{1+x}{1-x} \right) \left[1 + 3q_0 \frac{(1-x)^{\frac{1}{3}}}{1+x} \cos \gamma \right] \quad (4)$$

where we must specify

$$r \rightarrow 0 \Rightarrow x \rightarrow 0 \Rightarrow z \rightarrow 0 \Rightarrow t = t_0; H = H_0; R = R_0; K = K_0; a = a_0; q = q_0; r = D = D_L$$

$$\cos \gamma = 0 \Rightarrow z = z(x) \equiv z_0 \Rightarrow x = x(z_0) \Rightarrow r = r(z_0)$$

In fact the value $\cos \gamma = 0$ in eq. (4) leads naturally to another important convention, that is the introduction of z_0 to represent the **central redshift**, which must not be confused with $z(t_0) = 0$.

Moreover the previous eq. (4), with the H_0 and q_0 values obtained within the nearby Universe (paper II: $H_0 = 69.8 \pm 2.8 \text{ km s}^{-1} \text{ Mpc}^{-1}$; $q_0 \cong -0.0605$ from the data of Sandage & Tammann (1975)), allows a **numerical calculus of x** , that is of **the light-space r as a function of the observed z and γ** , as follows

$$x = x(z, \cos \gamma) = 3H_0 r / c \Rightarrow r = \frac{c \cdot x(z, \cos \gamma)}{3H_0} = r(z, \cos \gamma) \quad (5)$$

Note that $\cos \gamma = 0$ gives to $z_0 = 0.5$ an $x = 0.5$, that is $r \cong 716 \text{ Mpc}$.

2.2 D : Distance in the Hubble diagram and the h convention

In 1975 Sandage & Tammann published a paper (S&T: Paper V) in which an accurate data listing of nearby galaxies (mean depth of $\sim 28 \text{ Mpc}$) was tabled and reported in a famous wedge-shaped Hubble diagram, where the Hubble ratios appeared scattered between ~ 30 and $\sim 150 \text{ km s}^{-1} \text{ Mpc}^{-1}$. Another wedge-shaped velocity-distance diagram, with different symbols for different methods and a covered distance depth of about 200 Mpc , is that of Rowan-Robinson (1988); here the Hubble constant appears to lie in the range $50 - 80 \text{ km s}^{-1} \text{ Mpc}^{-1}$, with a current best value in the middle of this range.

Such a wedge feature of the original Hubble diagram is well represented by eq. (2) and (4). In fact, after putting

$$D = r \cdot \left(\frac{1+x}{1-x} \right) \quad (6)$$

we can transform eq. (2) into the **ECM Hubble law**

$$cz = [H_0 - a^*(x) \cos \gamma] \cdot D = [H_0 - a_0 X(x, \cos \gamma)] \cdot D = H_X \cdot D \quad (7)$$

being

$$a^*(x) = a_0 \cdot (1-x)^{\frac{1}{3}} / (1+x) \quad X(x, \cos \gamma) = \cos \gamma \cdot (1-x)^{\frac{1}{3}} / (1+x)$$

where both x and X are dimensionless variables (cf. paper V and VI); hence the above eq. (7) contains **an anisotropic angular coefficient**, that is

$$H_X = H_0 \left(1 - \frac{a_0}{H_0} X \right) \quad (8)$$

As in the very nearby Universe in practice $x \rightarrow 0$, here eq. (7) gives $a^* \simeq a_0$, that is $H_X(\gamma = 0^0) \cong 57 \text{ km s}^{-1} \text{ Mpc}^{-1}$ and $H_X(\gamma = 180^0) \cong 83 \text{ km s}^{-1} \text{ Mpc}^{-1}$ with $a_0 \cong 12.7 \text{ km s}^{-1} \text{ Mpc}^{-1}$ (paper V: section 4.6).

The MacLaurin Series applied to (6) and the ECM Hubble law (7) give D both in terms of a power series of the light-space r ,

$$D = r + 2\frac{3H_0}{c}r^2 + 2\frac{9H_0^2}{c^2}r^3 + \dots \quad (9)$$

and as a function of z_0 , that is the ratio between the central velocity cz_0 and the constant H_0 :

$$D = \frac{cz_0}{H_0} = D(z_0) \quad (10)$$

The eqs. (6)(9)(10) represent the **distance** D of the wedge-shaped Hubble diagram of eq. (7).

At the same time **the ECM Hubble law (7) is able to substantiate the powerful h convention** (Zeilik & Smith 1988) for large-scale surveys of radial distance D in H.u., by using a variable $h = h(X)$ tied to the ECM apparent anisotropy (cf. paper II, section 1.2) and the correct z , obtained after subtracting from the observed heliocentric redshift the kinematic component due to the entire motion of the Sun with respect to the Hubble flow traced by the CMB (Lorenzi 1993, 1999a, 2008, 2009). So we confirm the following useful formula:

$$D = \frac{cz}{100 \text{ km s}^{-1} \text{ Mpc}^{-1}} h^{-1} \quad \text{with} \quad h = \frac{H_X}{100 \text{ km s}^{-1} \text{ Mpc}^{-1}} \quad (11)$$

2.3 D_L : Luminosity distance and correlated absolute magnitude M

Papers V and VI have empirically confirmed the ECM even for Abell clusters of Richness 3 and Type Ia supernovae from SCP, up to a light-space distance r of $\sim 1000 \text{ Mpc}$. Here the luminosity distance D_L has been successfully represented by the following **ECM D_C multiple formula**

$$D_C = D(1+z) = \frac{xc}{3H_0} \left(\frac{1+x}{1-x} \right) (1+z) = \frac{cz(1+z)}{H_0} \left(1 - \frac{a_0}{H_0} X \right)^{-1} \quad (12)$$

Consequently, with $D_C \equiv D_L$ assumed, the distance D of the Hubble diagram can be simply inferred from the position

$$D = \frac{D_L}{1+z} \quad (13)$$

when one knows the absolute magnitude M , that is

$$M = m - 5 \log D_L - 25 \quad (14)$$

By combining the canonic eq. (14) in H.u. with (12) and (13), we can obtain the **ECM M equation**, written in a double form:

$$M = m - 5 \log \left[\frac{xc}{3H_0} \left(\frac{1+x}{1-x} \right) (1+z) \right] - 25 \quad (15)$$

$$M = m - 5 \log [cz(1 + z)] + 5 \log H_0 + \Delta - 25 \quad (16)$$

In (14)(15)(16) m and z are the observed magnitude and redshift within the Hubble flow; in (15) $x = x(z, \cos \gamma)$ from eq. (4); Δ of eq. (16) results to be a power series of $X(x, \cos \gamma)$, as follows

$$\Delta = 5 \log \left(1 - \frac{a_0}{H_0} X \right) = -\frac{5a_0}{H_0} \log e \cdot \left(X + \frac{a_0}{H_0} \frac{X^2}{2} + \frac{a_0^2}{H_0^2} \frac{X^3}{3} + \dots \right) \quad (17)$$

Eq. (16) can be simplified by introducing the central redshift z_0 corresponding to z of eq. (4) with $\cos \gamma = 0$, that is $H_X = H_0$. In this case, being

$$X \equiv 0 \Rightarrow \Delta = 0 \Rightarrow z = z_0 \Rightarrow m = m_0(z_0) \Rightarrow D_L = D_L(m_0) \quad (18)$$

, we also obtain the **ECM $M(z_0)$ equation**, in the form

$$M = m_0 - 5 \log [cz_0(1 + z_0)] + 5 \log H_0 - 25 \quad (19)$$

3. Construction of the ECM Hubble diagram of 398 SCP supernovae

The main aim of the present work is the application of the above formulae to the largest available sample of homogeneous datasets. The SCP "Union" SNe Ia compilation holds such a sample, bringing together data from 414 SNe (Kowalski et al 2008: Table 11) drawn from 13 independent datasets, of which 398 SNe have both the required redshifts z and blue magnitudes m_B^{\max} listed, while a wide subsample of 307 SNe Ia pass usability cuts. Note that here the redshifts z are referred to the CMB; hence they include the correction due to the standard motion of the Local Group, without taking into account the ECM 3K dipole able to generate a fictitious vector v_f (Lorenzi 1993, 1999a, 2008). As the involved correction to z is about 0.001 on average, the z of the distant supernovae in effect do not suffer an imprecise correction; it is different for the very nearby SNe, whose redshifts in the Hubble diagram should be corrected only for the Sun's velocity inside the Local Group (by the standard vector of S&T (1975)), because our LG belongs to a large local cosmic flow also running almost in the same direction (cf. p. 19 of paper I).

On the whole the present analysis aims directly to construct the ECM Hubble diagram, of course without using $\cos \gamma$, but showing in any case that the diagram's wedge-shape is due to the ECM dipole anisotropy. A further and crucial confirmation of the model is expected by introducing the supernova astronomical coordinates, that is to say $\cos \gamma$, into the ECM analysis both for SCP Union (Kowalski et al. 2008) and the SCP "Union2" shown at 2010 AAS (Rubin et al. 2010).

3.1 Search for a correlation between M_B and central redshift z_0

Initially the ECM Hubble law (7) was tested over the 398 SCP supernovae (Kowalski et al. 2008: Table 11), by assuming H_0 as the average Hubble ratio, that is

$$H_0 = \langle H_X \rangle = \left\langle \frac{cz}{D} \right\rangle \quad (20)$$

The procedure, based on the mean eq. (20) in H.u. with D derived from (13) and $D_L = 10^{0.2(m_B^{\max} - M_B) - 5}$, was applied to five large z bins of the Hubble flow, precautionally excluding the nearby SNe with $z < 0.05$; hence, once M_B or a resulting $H_0 \cong 70$ H.u. are fixed, the value of H_0 or M_B follow. Conditions and results of that first check are listed below, in Table 1.

Table 1

z bins	N	$\langle z \rangle$	$H_0 = H_0(M_B = -19.5)$	$M_B = M_B(H_0 \cong 70)$
$0.05 \leq z \leq 0.5$	145	0.334	62	-19.25
$0.25 \leq z \leq 0.75$	197	0.492	67	-19.41
$0.05 \leq z \leq 1.552$	308	0.568	70	-19.49
$0.5 \leq z \leq 1.0$	142	0.706	74	-19.63
$0.75 \leq z \leq 1.25$	67	0.916	81	-19.81

The strong variation of the H_0 value in the 4th column, corresponding to the assumed $M_B = -19.5$ (cf. paper VI), clearly rules out the possibility of a constant value of the SNe Ia absolute blue magnitude M_B . On the other hand the constant value of H_0 gives to SNe Ia a variable intrinsic luminosity, which clearly increases with depth or central redshift, according to the ECM.

Owing to the clear result in Table 1 and in order to construct a correlation between M_B and the central redshift z_0 according to (19), the same "z bins" procedure has been applied to a **normal ECM M equation**, that is eq. (16) with $H_0 = 70$ H.u. and $\langle \Delta \rangle = 0$ assumed, as follows

$$\langle M_B \rangle = \langle m_B^{\max} \rangle - 5 \langle \log [cz(1+z)] \rangle + 5 \log H_0 - 25 \quad (21)$$

In this case the check is more useful than the previous one, first of all because eq. (21) gives directly $\langle M_B \rangle$ with its standard deviation; furthermore the ECM eq. (21) seems to be statistically powerful, if the z scattering due to unsuitable corrections of Sun kinematics in the CMB is assumed to be neutralized like Δ by the normal point, apart from any anisotropies of SNe Ia distribution in the sky plus a H_0 imprecision of about ± 0.1 magnitudes. In other words eq. (21) seems able to produce M_B values correlated to the central redshift z_0 of eq. (19). Thus all the available SCP

SNe Ia of the Union 2008, 91 nearby SNe with $z \leq 0.05$ included, have been taken into account. Table 2 in the Appendix lists the results of the mean; it reports 30 normal points, including all the 398 SNe listed in Table 11 of the 2008 SCP paper (Kowalski et al. 2008) and corresponding to 30 "z bins". In particular the first 5 columns of Table 2 hold numerical values derived from the observed z and m_B^{\max} listed within the above SCP Union 2008; the values referring to each z bin are in the order: z range, number N of the SNe included in the normal point; unweighed mathematical mean $\langle m_B^{\max} \rangle$ of the observed SN blue magnitudes m_B^{\max} ; absolute magnitude $\langle M_B \rangle$ resulting from the normal ECM M equation (21) applied to the bin, with $H_0 = 70$ H.u. assumed; standard deviation s of the least square fitting carried out on the bin. The 6th column of Table 2 reports the mathematical mean $\langle z \rangle$ of the observed redshifts of the z bin, while the last columns, 7th, 8th, 9th, include three different distance values, corresponding to an assumed central redshift $z_0 \equiv \langle z \rangle$ with $H_0 = 70$ H.u.. These are in the order: value of the dimensionless variable $x = x(z_0)$, inferred as in (5) from the ECM z equation (4); value in Mpc of the light-space distance $r = r(z_0)$ connected to the x value by $x = 3H_0r/c$ according to procedure (5) applied to eq. (2) or (4); value in Mpc of the distance D of the wedge-shaped Hubble diagram, obtained with eq. (6) or (10), that is as the function $D = D(z_0)$ of the central redshift through $x(z_0)$.

The resulting normal points, plotted in Figure 1 as $\langle M_B \rangle$ versus $\langle z \rangle$, clearly point to a fitted trend line, whose equation formally should give for any z its M_B as a function of the central redshift z_0 , or the corresponding distance $D = cz_0/H_0$ as in Figure 2, if z_0 is assumed to refer to the line fitting the $\langle z \rangle$ points. The line equation below,

$$M_B(z_0) = A_0 + A_1z_0 + A_2z_0^2 = d_0 + d_1D + d_2D^2 = M_B(D) \quad (22)$$

, with $A_0 \cong -18.77$; $A_1 \cong -1.421$; $A_2 \cong +0.3589$ and $d_0 = A_0$; $d_1 = A_1H_0/c$; $d_2 = A_2H_0^2/c^2$, follows from the automatic fitting.

In the same way, according to procedure (5) applied to eq. (2) or (4) with $\cos \gamma = 0$, that is with $z = z_0$, an alternative plot of normal points $\langle M_B \rangle$ versus $x = x(z_0)$ or $r = r(z_0)$ can be constructed; it appears in Figure 3 and Figure 4, where the fitted trend line appears better represented by a third degree equation, that is

$$M_B(x) = B_0 + B_1x + B_2x^2 + B_3x^3 = C_0 + C_1r + C_2r^2 + C_3r^3 = M_B(r) \quad (23)$$

, with $B_0 \cong -18.78$; $B_1 \cong -0.4523$; $B_2 \cong -0.5338$; $B_3 \cong -2.006$ and $C_0 = B_0$; $C_1 = 3B_1H_0/c$; $C_2 = 9B_2H_0^2/c^2$; $C_3 = 27B_3H_0^3/c^3$, again obtained from the automatic fitting. Here the curve

agrees with that found in paper VI for 33 SNe Ia of K03 (cf. paper VI-integral version: Fig. 5), however with a systematic shift of about 0.3 magnitudes limited to the nearby Universe.

3.2 Construction of the Hubble diagram

The above equation (22), that expresses $M_B(D)$, has a crucial role in the construction of the SNe Ia Hubble diagram, which requires the distance D to combine with the observed redshift as cz . In fact it is now possible to extract numerically just the distance D from the canonic eq. (14), that becomes the following:

$$d_2 D^2 + d_1 D + d_0 = m_B^{\max} - 5 \log [D(1+z)] - 25 \quad (24)$$

The numerical solution point by point of eq. (24), here applied to 398 SNe Ia with z and m_B^{\max} listed in Table 11 of the SCP Union Compilation (Kowalski et al. 2008), gives the value of D . Once found, one can infer numerically also the corresponding values of the distance indicator x and the light-space distance r .

Finally, two resulting wedge-shaped Hubble diagrams in H.u. are obtained by plotting cz versus D for the 398 SNe, in Figure 5, and the 307 SNe passing usability cuts, in Figure 6. Here we look at the Hubble diagram of the Deep Universe. Table 3abcdefghi in the Appendix lists the values in H.u. of D (3rd column) and cz (2nd column) of 249 SNe Ia (1st column: Name), lying in the distance range $800 \text{ Mpc} < D < 8000 \text{ Mpc}$, from the 307 SNe selected by the SCP Union.

4. ECM analysis of the wedge-shaped Hubble diagram

The diagrams in Fig. 5 and Fig. 6 have a wedge shape, whose amplitude with increasing depth is very large, indeed. In order to verify the accordance with the model, it is necessary to compare the observed wedge shape to the calculated one. In practice we should carry out an (O-C) procedure. That has been done by calculating the wedge amplitude foreseen by the ECM Hubble law (7) through a numerical **simulation** of the maximum scattering of cz around the central value cz_0 . To this end, let us analyse the observed Hubble flow or CM as follows:

$$z_0 = \frac{\lambda_0 - \lambda_e}{\lambda_e} = \frac{T_e}{T_0} - 1 \quad (25)$$

$$cz = cz_0 + c\Delta z_0 \quad (26)$$

$$\Delta z_0 = -\frac{T_e}{T_0} \left(\frac{\Delta T_0}{T_0 + \Delta T_0} \right) \quad (27)$$

As the **ECM** gives

$$cz_0 = H_0 D \quad c\Delta z_0 = -a_0 D X \quad (28)$$

, after fixing x , then r and D , solely the dimensionless X varies owing to the variation of $\cos \gamma$ between 1 and -1 . In this case:

$$-(1-x)^{\frac{1}{3}}/(1+x) \leq X \leq (1-x)^{\frac{1}{3}}/(1+x) \quad (29)$$

$$c\Delta z = c\Delta(\Delta z_0) = -a_0 D \Delta X \quad (30)$$

$$r = \frac{cx}{3H_0} \quad cz_0 = \frac{cx}{3} \left(\frac{1+x}{1-x} \right) \quad D = \frac{cx}{3H_0} \left(\frac{1+x}{1-x} \right) \quad (31)$$

$$(\Delta X)^{\max} = 2(1-x)^{\frac{1}{3}}/(1+x) \quad (32)$$

$$c|\Delta z|^{\max} = a_0 D (\Delta X)^{\max} \quad (33)$$

Now we add to the above **formulae** the following ones, which practically, being based solely on the eqs. (25)(26)(27), are **unaffected by the ECM** (cf. section 6 of paper VII).

$$\Delta T_0 = \Delta T_D \cos \gamma \quad (34)$$

$$\frac{\Delta z_0}{1+z_0} = -\frac{\Delta T_0}{T_0 + \Delta T_0} \quad (35)$$

$$\gamma = 0 \Rightarrow \frac{\Delta z_0}{1+z} = -\frac{\Delta T_0}{T_0} \equiv \frac{v_f}{c} \Rightarrow v_f = \frac{c\Delta z_0}{1+z} \quad (36)$$

The last equation of (36) gives the value of the fictitious velocity v_f observed towards the expansion center. Its value in H.u., obtained **within the ECM**, is listed in the 7th column of Table 4, while the previous 5 columns present the other simulated values in H.u. of $r, cz_0, D, (\Delta X)^{\max}, c|\Delta z|^{\max}$ from the above eqs. (31)(32)(33) corresponding to the x value of the first column. The last row of Table 4, where $x = 0.999999225$, reports the **ECM values extrapolated to the CMB**, whose fictitious velocity results to be only of the order -250 km s^{-1} . Curiously this value, that is in accordance with the observed 3K anisotropy and a local cosmic flow of about 530 km s^{-1} (cf. Lorenzi 1993, 1999a, 2008), is the same of the nearby Universe at $D \cong 20 \text{ Mpc}$, while at $D \cong 10000 \text{ Mpc}$ the corresponding value of v_f reaches a maximum of about -13000 km s^{-1} .

On the whole, the ECM simulation is able to reproduce the variable wedge-shape of the Hubble diagram at different depths, as summarized in the table below.

Table 4

x	r	cz_0	D	$(\Delta X)^{\max}$	$c \Delta z ^{\max}$	v_f
0.00070	0.9993	70	1	1.998	25	-13
0.00691	9.865	700	10	1.982	252	-126
0.013633	19.46	1400	20	1.964	499	-248
0.026569	37.93	2800	40	1.931	981	-487
0.038883	55.51	4200	60	1.900	1448	-716
0.050637	72.29	5600	80	1.871	1901	-936
0.061884	88.34	7000	100	1.844	2342	-1148
0.342820	489.4	70000	1000	1.295	16445	-6818
0.485378	692.9	140000	2000	1.079	27407	-9642
0.631939	902.1	280000	4000	0.8783	44617	-11997
0.710716	1015	420000	6000	0.7732	58918	-12793
0.760902	1086	560000	8000	0.7049	71622	-13029
0.7959346	1136	700000	10000	0.6556	83266	-13026
0.9	1285	1708817	24412	0.4886	151476	-11747
0.99	1413	19687373	281248	0.2165	773401	-5915
0.999999225	1427.582	$\simeq 2.6 \times 10^{11}$	$\simeq 3.7 \times 10^9$	0.0092	$\simeq 4.3 \times 10^8$	-250

Finally, Figure 7 and Figure 8 present two plots of the results in Table 4: the former refers to the nearby cosmic region with $D \leq 80 \text{ Mpc}$ and the latter to the Deep Universe with $D \leq 8000 \text{ Mpc}$. We obtain two simulated ECM Hubble diagrams in H.u., where the plotted points corresponding to each tabled D are the central cz_0 , the upper $cz_0 + \frac{c|\Delta z|^{\max}}{2}$ and the lower $cz_0 - \frac{c|\Delta z|^{\max}}{2}$. From their comparison, it results clearly that the wedge amplitude has to decrease with depth, until $H_X \rightarrow H_0$ for $x \rightarrow 1$.

5. Conclusions

This paper validates the wedge-shaped Hubble diagram predicted by the expansion center model. In fact the diagrams of the Deep Universe in Fig. 5 and Fig. 6 are in good accordance with that simulated in Fig. 8, as the observed amplification is certainly due to various sources of background noise. Therefore this 9th ECM contribution, based above all on a large sample of SCP

data obtained in space with HST, is further confirmation of the cosmic expansion center, following the ground-based astronomical proof collected in about half a century.

At this point one cannot desist from pressing the international astronomical community to pronounce itself once and for all on the subject. In conclusion the author extends an invitation to all astronomers to analyse independently the presented new wedge-shaped Hubble diagram, in order to confirm, or confute, the dipole anisotropy of the Hubble ratio cz/D at any cosmic depth.

Fig. 1: - SNe Ia absolute B magnitudes versus central redshift based on the ECM from SCP Union data

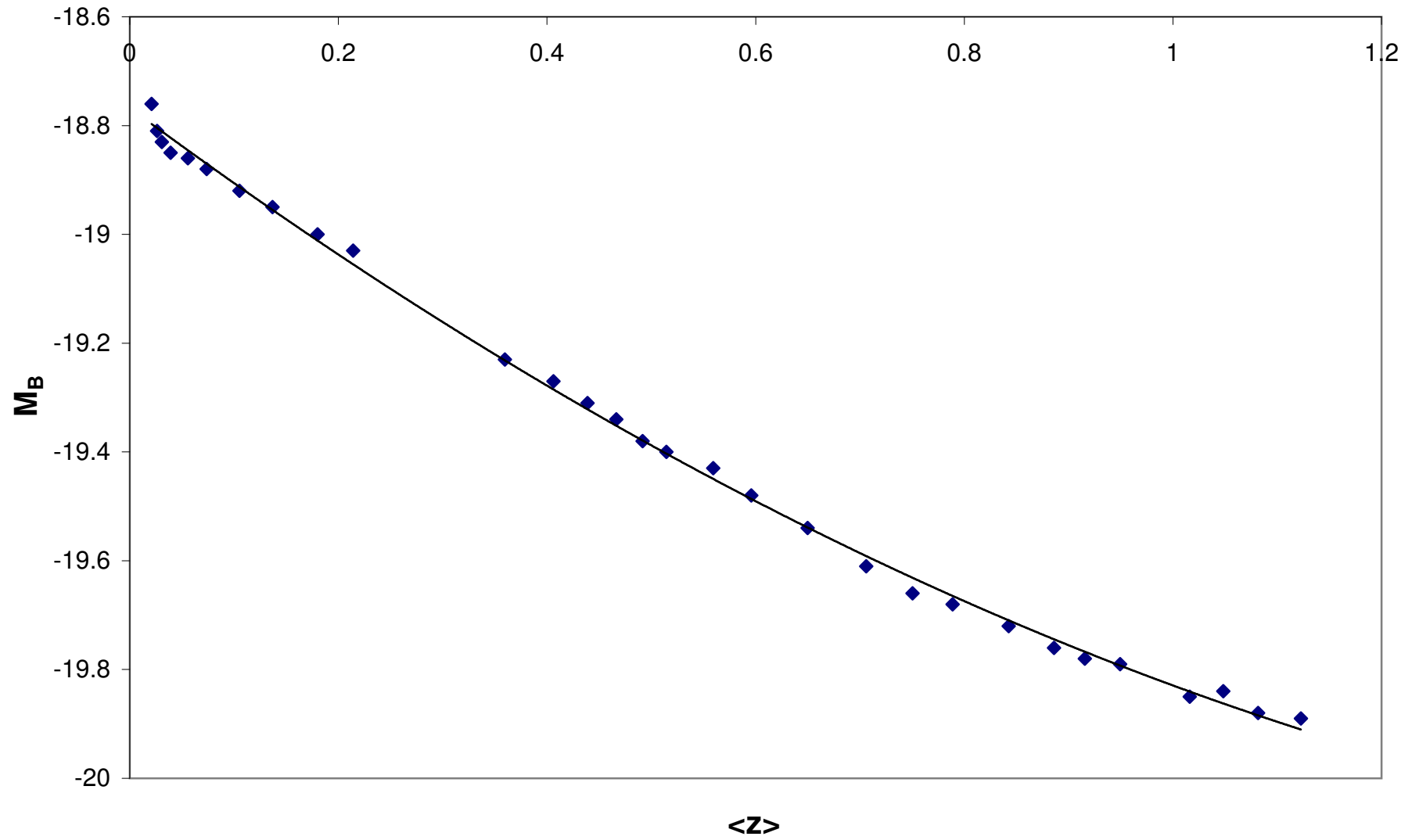


Fig. 2: - SNe Ia absolute B magnitudes versus distance D based on the ECM from SCP Union data

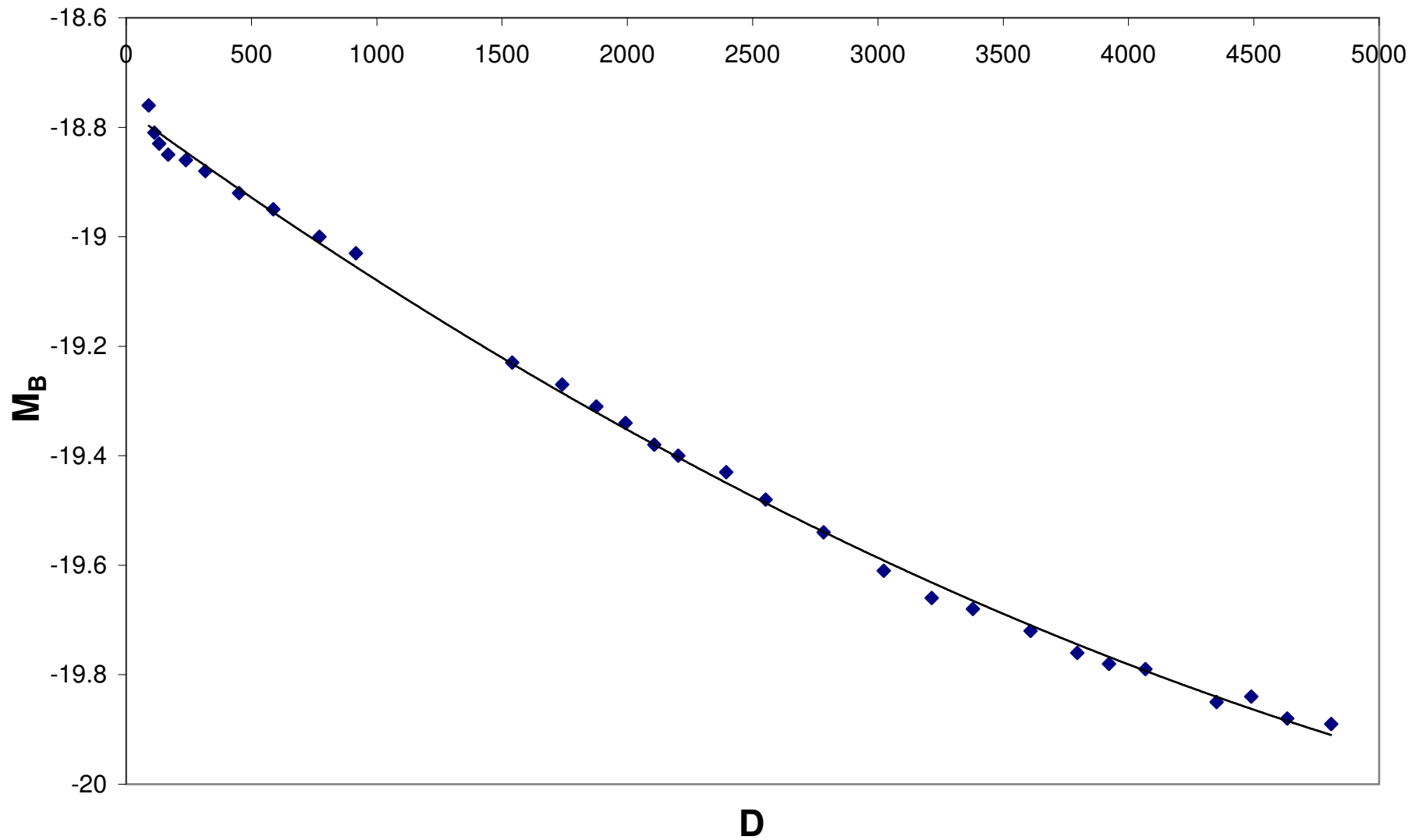


Fig. 3: - SNe Ia absolute B magnitudes versus the distance indicator x based on the ECM from SCP Union data

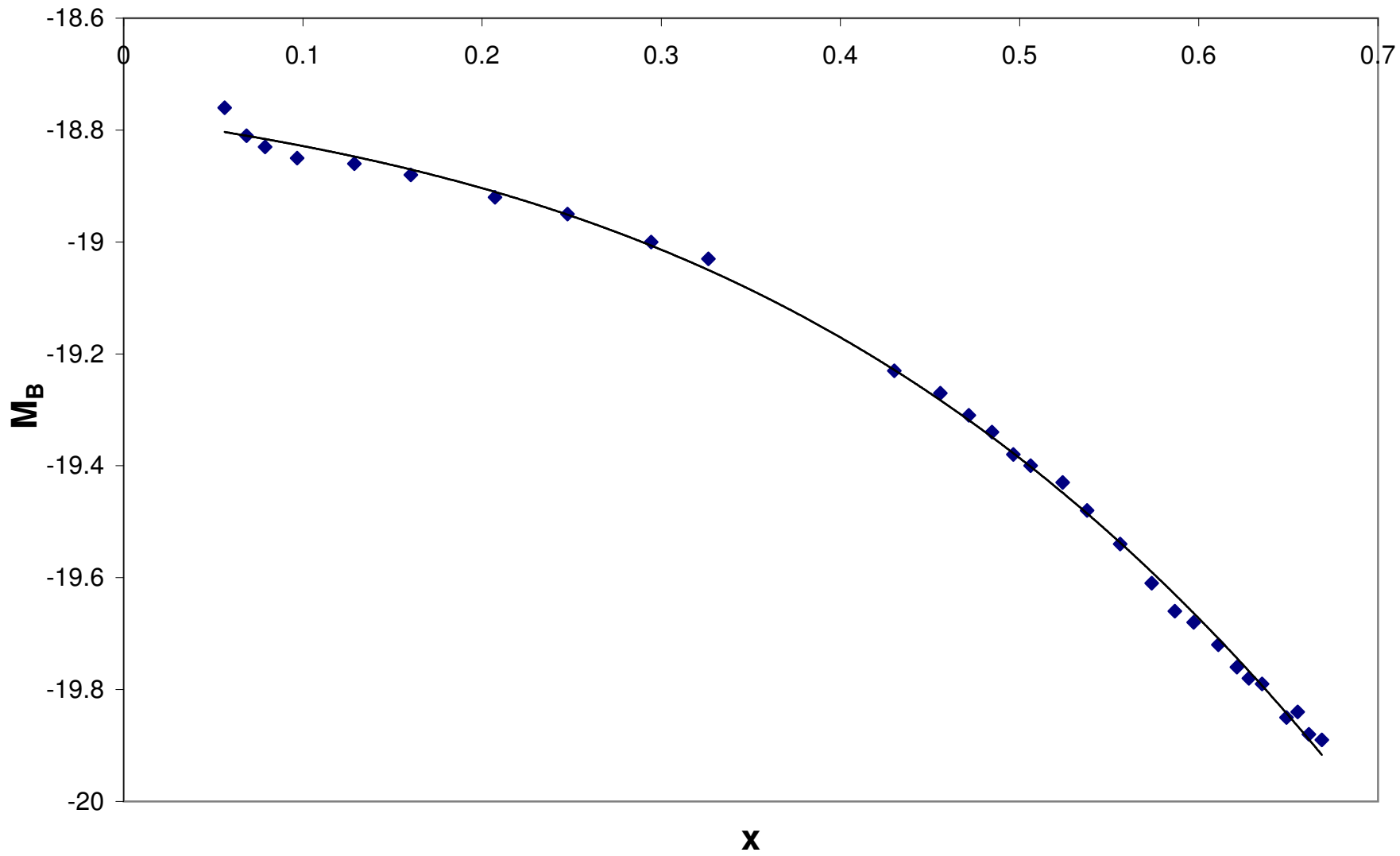


Fig. 4: - SNe Ia absolute B magnitudes versus light-space distance r based on the ECM from SCP Union data

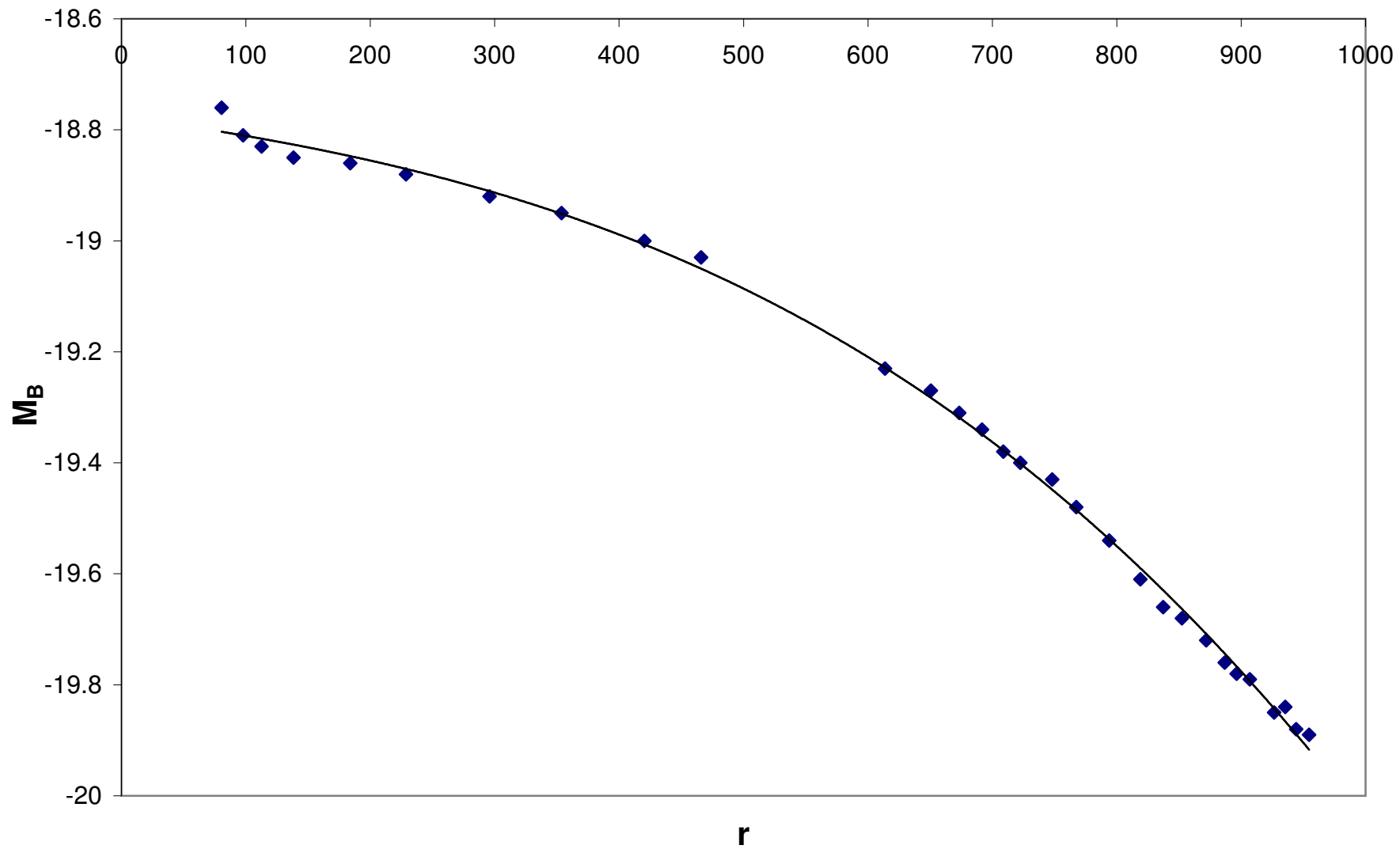


Fig. 5: - New Hubble diagram of 398 SCP supernovae

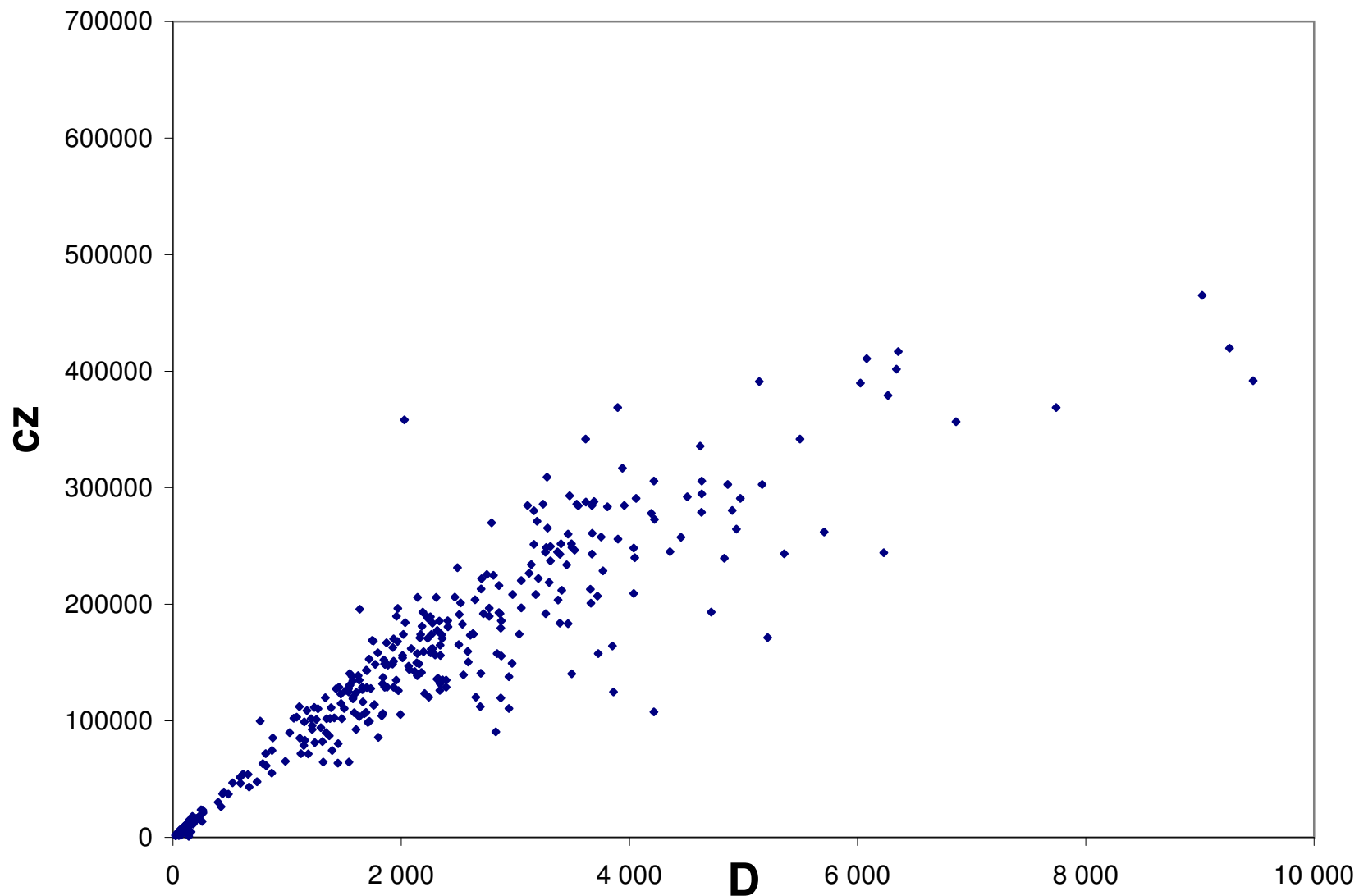


Fig. 6: - New Hubble diagram of 307 SCP supernovae

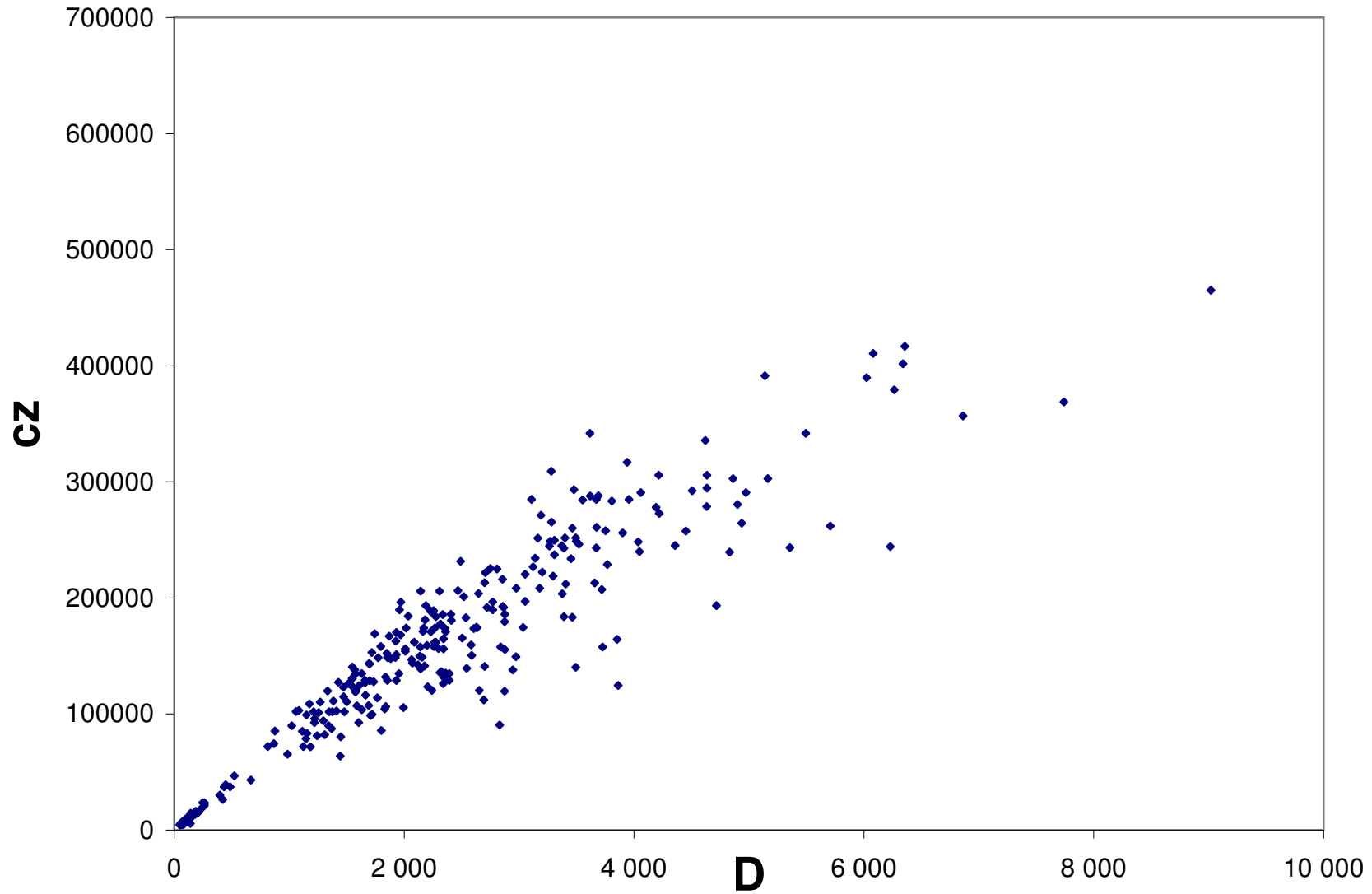


Fig. 7: - ECM Hubble diagram of the Nearby Universe by a simulation

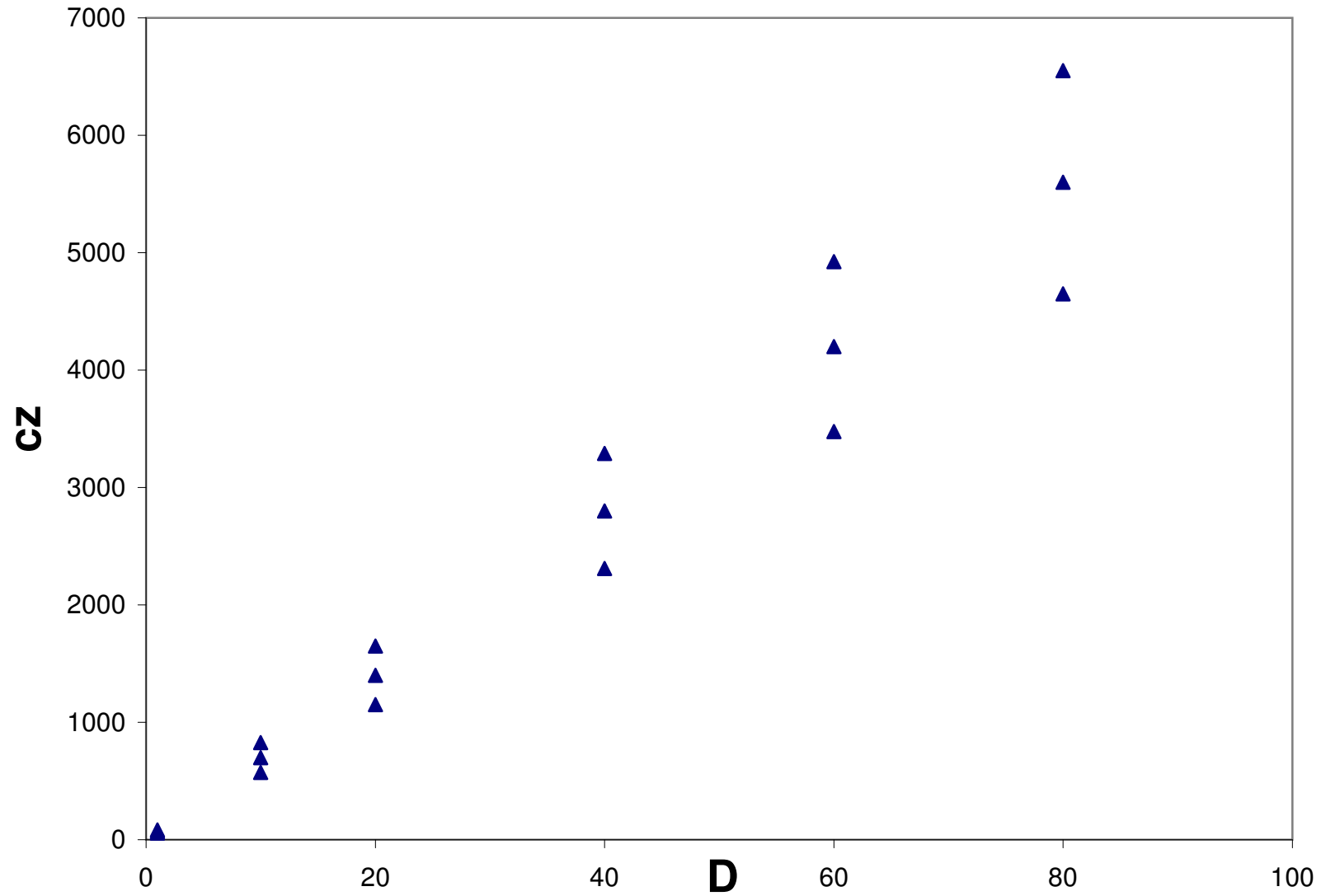
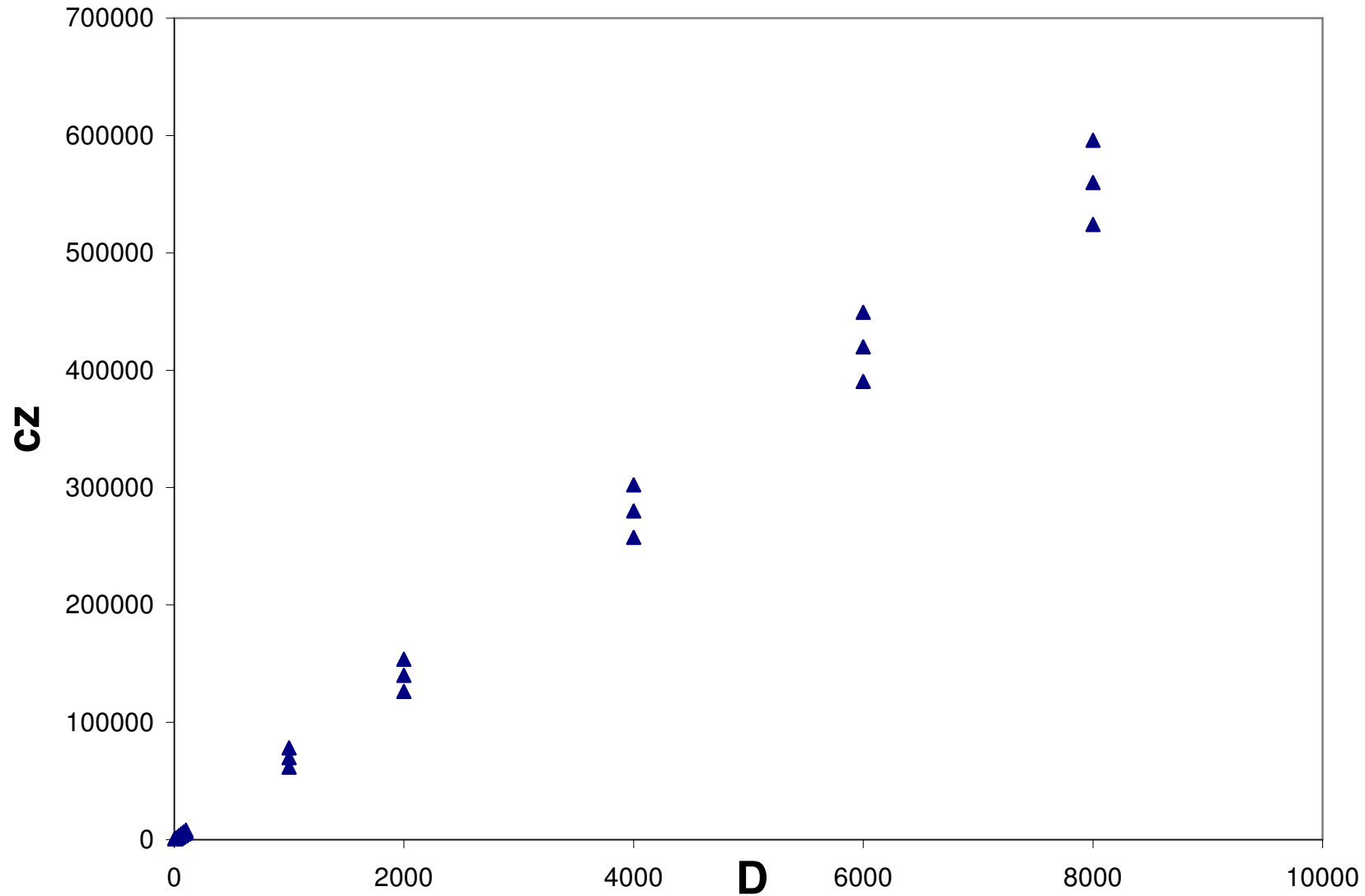


Fig. 8: - ECM Hubble diagram of the Deep Universe by a simulation



Acknowledgements

This work was made possible thanks to the SCP Union Compilation. The author would like to thank all the members of the SCP team, in particular for making the SNe data available on line in "arXiv:0804.4142v1 [astro-ph] 25 Apr 2008".

Special acknowledgements are reserved for the Local Organizing Committee of SAI2010 at Capodimonte Astronomical Observatory in Naples, both for the successful meeting and all the kind attention and support given to the present contribution.

A final word of gratitude goes to a dear friend Francesco Chiapello for all his encouragement.

REFERENCES

- Bahcall, N.A. and Soneira, R.M. 1982, ApJ 262, 419
- Knop, R.A. et al. 2003, ApJ 598, 102 (K03)
- Kowalski, M. et al. 2008, arXiv:0804.4142v1 [astro-ph] 25 Apr 2008→ApJ 686, 749
- Lorenzi, L. 1989, Contributo N. 0, CSA-Mondovì, Italy (unpublished)
- 1991, Contributo N. 1, CSA-Mondovì, Italy
- 1993, in 1995 MemSAIt, 66, 249
- 1999a, arXiv:astro-ph/9906290v1 17 Jun 1999,
in 2000 MemSAIt, 71, 1163 (paper I: reprinted in 2003, MemSAIt, 74)
- 1999b, arXiv:astro-ph/9906292v1 17 Jun 1999,
in 2000 MemSAIt, 71, 1183 (paper II: reprinted in 2003, MemSAIt, 74)
- 2002, in 2003 MemSAIt, 74, 480 (paper III-partial version),
http://sait.oat.ts.astro.it/MSAIIt740203/PDF/poster/39_lorenzil01_long.pdf
(paper III-integral version)
- 2003a, MemSAIt Suppl. 3, 277 (paper IV)
- 2003b, MemSAIt Suppl. 3,
http://sait.oat.ts.astro.it/MSAIS/3/POST/Lorenzi_poster.pdf (paper V)
- 2004, MemSAIt Suppl. 5, 347 (paper VI)
- 2008, www.sait.it, Archivio Eventi, 2008-LII Congresso Nazionale della SAIt,
<http://terri1.oa-teramo.inaf.it/sait08/slides/I/ecmcm9b.pdf> (paper VII)
- 2009, www.sait.it, Archivio Eventi, 2009-LIII Congresso Nazionale della SAIt,
<http://astro.df.unipi.it/sait09/presentazioni/AulaMagna/08AM/lorenzi.pdf>
(paper VIII)
- Perlmutter, S., et al. 1999, ApJ 517, 565 (P99)
- Rowan-Robinson, M. 1988, Space Science Review 48, 1
- Rubin, D. et al. 2010, SCP "Union 2" Shown at 2010 AAS
- Sandage, A., Tammann G.A. 1975, ApJ 196, 313 (S&T: Paper V)
- Zeilik, M., Smith, E.v.P. 1987, Introductory Astronomy and Astrophysics,
CBS College Publishing

APPENDIX

Table 2

z range	N	$\langle m_B^{\max} \rangle$	$\langle M_B \rangle$	s	$\langle z \rangle$	x	r	D
$z \leq 0.05$	91	15.69	-18.76 ± 0.09	0.848	0.0210	0.0563	80.4	90.0
$z \leq 0.10$	103	15.97	-18.81 ± 0.09	0.817	0.0262	0.0685	97.8	112.2
$z \leq 0.15$	108	16.15	-18.83 ± 0.08	0.802	0.0308	0.0789	112.6	131.9
$z \leq 0.20$	115	16.41	-18.85 ± 0.08	0.785	0.0392	0.0968	138.2	167.8
$z \leq 0.25$	126	16.85	-18.86 ± 0.07	0.763	0.0556	0.1287	183.8	238.1
$z \leq 0.30$	137	17.25	-18.88 ± 0.07	0.741	0.0738	0.1602	228.7	316.0
$z \leq 0.35$	156	17.85	-18.92 ± 0.06	0.727	0.1052	0.2072	295.8	450.4
$z \leq 0.40$	177	18.41	-18.95 ± 0.06	0.712	0.1369	0.2477	353.6	586.5
$z \leq 0.45$	208	19.06	-19.00 ± 0.05	0.684	0.1800	0.2944	420.3	771.0
$z \leq 0.50$	235	19.52	-19.03 ± 0.05	0.662	0.2141	0.3263	465.8	917.1
$0.05 \leq z \leq 0.55$	167	22.10	-19.23 ± 0.04	0.420	0.3595	0.4300	613.8	1540
$0.10 \leq z \leq 0.60$	174	22.54	-19.27 ± 0.04	0.436	0.4062	0.4557	650.5	1740
$0.15 \leq z \leq 0.65$	191	22.74	-19.31 ± 0.04	0.438	0.4380	0.4717	673.4	1876
$0.20 \leq z \leq 0.70$	199	22.90	-19.34 ± 0.04	0.447	0.4663	0.4846	691.8	1993
$0.25 \leq z \leq 0.75$	197	23.03	-19.38 ± 0.03	0.426	0.4919	0.4965	708.8	2107
$0.30 \leq z \leq 0.80$	197	23.14	-19.40 ± 0.03	0.420	0.5144	0.5061	722.5	2203
$0.35 \leq z \leq 0.85$	191	23.35	-19.43 ± 0.03	0.405	0.5592	0.5240	748.1	2394
$0.40 \leq z \leq 0.90$	180	23.50	-19.48 ± 0.03	0.362	0.5958	0.5376	767.5	2552
$0.45 \leq z \leq 0.95$	162	23.71	-19.54 ± 0.03	0.352	0.6498	0.5561	793.9	2783
$0.50 \leq z \leq 1$	142	23.90	-19.61 ± 0.03	0.330	0.7059	0.5737	819.0	3023
$0.55 \leq z \leq 1.05$	125	24.05	-19.66 ± 0.03	0.316	0.7505	0.5866	837.4	3214
$0.60 \leq z \leq 1.10$	105	24.19	-19.68 ± 0.03	0.306	0.7889	0.5971	852.4	3379
$0.65 \leq z \leq 1.15$	86	24.36	-19.72 ± 0.04	0.303	0.8425	0.6108	872.0	3609
$0.70 \leq z \leq 1.20$	73	24.49	-19.76 ± 0.04	0.343	0.8860	0.6212	886.8	3795
$0.75 \leq z \leq 1.25$	67	24.58	-19.78 ± 0.05	0.362	0.9156	0.6279	896.4	3922
$0.80 \leq z \leq 1.30$	60	24.68	-19.79 ± 0.05	0.369	0.9494	0.6353	906.9	4067
$0.85 \leq z \leq 1.35$	47	24.84	-19.85 ± 0.06	0.379	1.0161	0.6489	926.4	4351
$z \geq 0.85$	51	24.95	-19.84 ± 0.06	0.378	1.0484	0.6552	935.4	4490
$z \geq 0.9$	43	25.01	-19.88 ± 0.06	0.380	1.0817	0.6614	944.2	4633
$z \geq 0.95$	34	25.13	-19.89 ± 0.07	0.407	1.1228	0.6687	954.6	4809

Table 3a

Name	cz	D
1996h	185871	2407
1996i	170882	2360
1996j	89938	1343
1996k	113921	1766
1996u	128911	1659
1995ao	71950	1122
1995ap	89938	1023
1996t	71950	813
1997ce	131909	1838
1997cj	149896	2137
1997ck	290799	4058
1995k	143601	1695
1997ap	248828	3497
1997am	124714	1541
1997aj	174179	2018
1997ai	134907	1956
1997af	173580	2606
1997ac	95934	1221
1997r	196964	3053
1997p	141502	2178
1997o	112122	2693
1997h	157691	2140
1997g	228742	3768
1997f	173880	2354
1996cn	128911	2393
1996cm	134907	2393
1996cl	248228	4037
1996ck	196664	2772
1996ci	148397	1773
1996cg	146898	2066

Table 3b

Name	cz	D
1996cf	170882	2232
1995ba	116319	1664
1995az	134907	1631
1995ay	143900	2072
1995ax	184372	2035
1995aw	119917	1335
1995at	196364	1971
1995as	149297	2972
1995ar	139404	2545
1995aq	135806	2313
1994g	127412	1429
1999fw	83342	1156
1999fn	143001	1698
1999fm	284803	3107
1999fk	316881	3939
1999fj	244631	3264
1999ff	136406	2324
2002ad	154093	2011
2002ab	126812	1660
2002aa	283604	3808
2002x	257522	4451
2002w	309086	3279
2001kd	280606	4900
2001jp	158290	1796
2001jn	193366	4717
2001jm	293197	3476
2001jh	265316	3283
2001jf	244331	6230
2001iy	170282	1933
2001ix	213152	2700

Table 3c

Name	cz	D
2001iw	101809	1347
2001iv	118868	1577
2001hy	243431	5357
2001hx	239534	4832
2001hu	264417	4938
2001hs	249727	3307
2001fs	262019	5706
2001fo	231440	2492
2000fr	162787	1927
1998bi	224844	2808
1998be	191867	2865
1998ba	128911	1933
1998ay	191867	2721
1998ax	148997	2156
1998aw	131909	2342
1998as	106426	1840
1997ez	233838	3451
1997eq	161888	2089
1997ek	257822	3752
04Eag	305788	4635
04Gre	341764	3617
04Man	256023	3900
04Mcg	410716	6080
04Omb	292298	4507
04Pat	290799	4973
04Rak	221846	2706
04Sas	416712	6355
04Yow	137905	2945
05Fer	305788	4214
05Gab	335768	4620

Table 3d

Name	<i>cz</i>	<i>D</i>
05Lan	368745	7739
05Red	356753	6863
05Spo	251526	3163
05Str	302791	4862
05Zwi	156192	2011
2002dc	142401	2119
2002dd	284803	3955
2002fw	389730	6024
2002hp	391229	5139
2002hr	157691	3727
2002kd	220347	3053
2002ki	341764	5495
2003az	379237	6265
2003dy	401722	6339
2003eq	251826	3492
03D4au	140303	3494
04D4bk	251826	3400
04D3nr	287801	3619
04D3lu	246370	3520
04D3ki	278807	4632
04D3gt	135206	2361
04D3do	182873	2537
04D3cp	248828	3271
04D2gp	211953	3407
04D2fp	124414	1606
04D1ag	166984	1871
03D4fd	237136	3308
03D4cz	208356	3178
03D4at	189769	2772
03D3bh	74528	867

Table 3e

Name	<i>cz</i>	<i>D</i>
03D3af	159490	2582
03D1fc	99231	1151
03D1bp	103728	1632
04D4dw	288101	3690
04D4an	183773	3391
04D3nh	101989	1376
04D3lp	294696	4635
04D3is	212853	3659
04D3fq	218849	3297
04D3df	140903	2699
04D3co	185871	2877
04D2gc	156192	2343
04D2cf	110623	1501
03D4gl	171182	2163
03D4dy	181075	2182
03D4cy	277938	4192
03D4ag	85441	875
03D3ba	87300	1369
03D1gt	164286	3852
03D1ew	260220	3463
03D1ax	148697	1924
04D4dm	243132	3672
04D3oe	226643	3122
04D3nc	244930	3371
04D3ks	225444	2750
04D3hn	165366	2505
04D3fk	107266	1691
04D3dd	302791	5164
04D2ja	222146	3203
04D2gb	128911	1855

Table 3f

Name	<i>cz</i>	<i>D</i>
04D1ak	157691	2840
03D4gg	177477	2316
03D4di	271312	3191
03D4cx	284503	3552
03D3cd	138114	1570
03D3ay	111193	1385
03D1fq	239834	4047
03D1co	203559	3375
03D1aw	174389	2633
04D4bq	164886	2342
04D3ny	242832	3390
04D3ml	284803	3671
04D3kr	101120	1256
04D3gx	272811	4219
04D3ez	78845	1147
04D3cy	192767	2857
04D2iu	207157	3719
04D2fs	107026	1588
04D1aj	216150	2856
03D4gf	174179	2266
03D4dh	187910	2236
03D4cn	245230	4356
03D3aw	134607	1577
03D1fl	206257	2469
03D1cm	260820	3673
03D1au	151185	1933
b010	177177	2318
b013	127712	1734
b016	98632	1707
d033	159190	2197

Table 3g

Name	<i>cz</i>	<i>D</i>
d058	174779	2630
d084	155592	2877
d085	120217	1580
d087	101930	1212
d089	130710	1550
d093	108825	1175
d097	130710	1550
d117	92636	1605
d149	102529	1413
e029	99531	1722
e108	140603	1550
e132	71650	1186
e136	105527	1994
e138	183473	3463
e140	189169	2228
e147	193366	2189
e148	128611	1700
e149	148997	1855
f011	161588	2264
f041	168184	1968
f076	122915	1472
f096	123515	2205
f216	179576	2874

Table 3h

Name	<i>cz</i>	<i>D</i>
f231	185572	2335
f235	126512	1525
f244	161888	2276
f308	120217	2242
g005	65355	986
g050	189769	1959
g052	114821	1474
g055	90537	2830
g097	101930	1481
g120	152894	1720
g133	126213	2340
g142	119617	2874
g160	147798	1884
g240	205957	2143
h283	150496	2587
h300	205957	2307
h319	148397	1858
h323	180775	2411
h342	126213	1517
h359	104328	1831
h363	63856	1445
h364	103129	1084
k396	81244	1242

Table 3i

Name	<i>cz</i>	<i>D</i>
k411	169083	1744
k425	82143	1309
k430	174479	3034
k441	203859	2648
k448	120217	2655
k485	124714	3861
m027	85741	1801
m062	94135	1297
m138	174179	2171
m158	138804	2142
m193	102229	1058
m226	201161	2520
n256	189169	2256
n258	156492	2298
n263	110324	1270
n278	92636	1219
n285	158290	2258
n326	80344	1448
p454	208356	2976
p455	85141	1113
p524	152295	1849
p528	234138	3141
p534	183773	2275